ABSTRACT

Title of Thesis: ADVANCED BLISTER TESTING WITH PREDEFINED AREA *(AND FLEXIBLE CONSTRAINER)*

David Rosen, Master of Science, 2014

Thesis directed by: Professor Bongtae Han
Department of Mechanical Engineering

An advanced blister test using a predefined blister area is employed to determine the adhesion strength (energy release rate) as well as characterize the flexural modulus of polymer material. The predefined blister area allows for a low adhesion precrack area, defining an initial constant blister area and the modulus determined from each experiment negates the effect of uncertainties associated with the polymer modulus. Ideal specimens with epoxy coatings of various thickness are analyzed using the proposed setup. After measuring the properties at time zero the coatings are subjected to accelerated testing conditions (high temperature/ humidity storage) and the degradations of the coating properties are documented. The modulus increases significantly after thermal aging but the adhesion strength is determined accurately by accounting for the effect of the modulus quantitatively.

ADVANCED BLISTER TESTING WITH PREDEFINED AREA

by

David Ian Rosen

Thesis submitted to the Faulty of the Graduate School of the
University of Maryland, College Park in partial fulfillment
of the requirements for the degree of
Master of Science
2014

Advisory Committee:

Professor Bongtae Han, Chair
Professor Abhijit Dasgupta
Associate Professor Patrick McCluskey

ACKNOWLEDGEMENTS

I would like to thank those of who have made my journey leading up to this thesis possible. First and foremost, I thank Dr. Han for his support and guidance during my graduate and later undergraduate years. Your passion for to watch me learn and succeed has strongly motivated me to try to develop into the best engineer I could come. I will cherish both the engineering knowledge and life philosophies you have shared with me throughout my lifetime.

A big thank you to Kenny for assisting me in completing this work. Your assistance with the FEM modeling, specimen preparation procedure, and revision of this thesis is appreciated tremendously. Also, thank you to my other lab mates over the years: Dae-Suk, Yong, Bulong, Sean, Stephan, Michelle, and Brian. There was not a single day over the past few years that I would not learn something from you all. Thank you for being great friends.

Thank you to my parents, Barbara and Ken, as well as my sister Janis for supporting me through this experience. Without your constant support and love, I would not have been able to make it this far in my academic pursuit.

Finally, thank you to all of my friends. Your patience, encouragement, and excitement has motivated me greatly.

TABLE OF CONTENTS

LIST OF TABLES

LIST OF FIGURES

CHAPTER 1: HISTORY OF ADHESION TESTING

1.1 Description of Adhesion

Depending on the system examined, adhesion is generally thought of in two contexts: the molecular level and the mechanical level. On the molecular level, two smooth surfaces may experience an attractive force if brought within close proximity to one another, typically a separation of 1 to 10 nm. This attractive force is not magnetic or electrostatic in nature, rather it is independent. This force is molecular adhesion. The magnitude of opposite force required to separate two materials is called the adhesion force [1].

An example of mechanical adhesion is when a material fills the voids of another it comes in contact with, promoting interlocking. This interaction between the two materials also causes yields an attractive force, yielding another definition of adhesion. Similar to the molecular case, the magnitude of force required to separate the materials is the adhesion force. Typically with engineering materials, one is more concerned with the mechanical adhesion. Since most surfaces do not tend to be perfectly smooth on the molecular level, it is reasonable to hypothesize that the molecular adhesion does not typically make large contributions to the overall adhesion strength of two materials.

1.2 Energy Release Rate

To characterize the adhesion strength a concept known as the energy release rate can be employed. Consider a bimaterial body that has an interfacial crack and is experiencing

monotonic loading. As the load increases, so does the stress around the crack tip until finally a critical loading condition is reached and the crack delaminates. When the crack delaminates two key events happen: new surface area is created, and some of the stored energy in the body is released. This release of stored energy to create new surface area is defined as the energy release rate [2].

1.3 Adhesion Issues in Electronic Packages

Within the electronics packaging community, adhesion strength is of high importance. Within an electronic device, failure at the chip level could result in an entire system failure or malfunction, thus jeopardizing the reliability of the device as a whole. Currently, there is a trend toward smaller and thinner electronic devices as consumers drive the market toward ultra-portable devices. On the chip level, components consequently become less rigid and more prone to mechanical deformations via thermal warpage. An adhesive's mechanical properties are also prone to change after many cycles of thermal fatigue. Environmental conditions also affect the adhesion strength of materials, namely high heat and high humidity conditions. Having the ability to quantify the adhesion strength of chip components, such as die attach films, will allow valuable insight in how different components should be designed with reliability in mind.

1.4 Current Adhesion Tests

Four commonly used methods to determine adhesion strength are the double cantilever beam test, the peel test, the three/four point bend test, and the standard blister test. Each has its own set of advantages and disadvantages.

1.4.1 Double Cantilever Beam Test

The double cantilever beam test is a commonly used method to measure the adhesion strength between wafer materials. The experimental procedure involves forcing a thin blade between the two layers of wafer and determining the resulting length of the crack (*a)* via laser sensor. A schematic of this experimental setup can be seen in Figure 1-1 below. Although shown to be accurate, the experimental is difficult to perform due the possibility of damaging or breaking a wafer upon contact with the blade. This test is also very sensitive to crack length, and therefore will need an accurate crack length measurement method in-situ during testing. In addition, since only the edges of the adhesive layer are exposed to environmental conditions. For humidity degradation tests, a common problem is the amount of degradation not being even along the width of the specimen [3, 4].

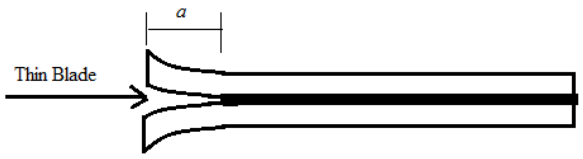

Figure 1-1. Schematic of double cantilever beam test.

1.4.2 Peel Test

Another commonly used adhesion test for flexible adhesives is the peel test. The experimental procedure to conduct this test is considered to be the simplest of those discussed. A flexible adhesive is stripped from a substrate in a controlled manner, usually by a tension loading device. The crosshead is configured so that it undergoes a

constant displacement until about half of the bond length. By determining the average pull force (*F)* along this length, the adhesion strength can be quantified. A schematic of the 180° test can be seen in Figure 1-2. Although testing adhesives in this matter is simple to do, the analysis is quite difficult due to the complex stress states that arise when the adhesive undergoes this configuration. A full description of the nonlinear material properties of the film is required. In addition, the test is very sensitive to parameters such as peel angle, width, and thickness of the adhesive. Finally, the peel test does not provide any insight on the adhesive's mechanical properties. Rather, it only indicates its resistance to peeling forces [5, 6].

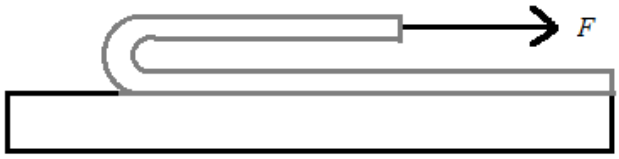

Figure 1-2. Schematic of the 180° pull test.

1.4.3 Three/ Four Point Bend Tests

Three point bend tests are also used to determine adhesion strength. A benefit of these tests is that they can be configured to load the specimen in high shear configurations. This steers away from the possibility of obtaining data that corresponds to the toughness of the adhesive. Typically, these test specimens involve two rectangular metal panels with an adhesive material sandwiched in between (Figure 1-3a). A small precrack area is cut through the top layer, promoting an initial failure point. The specimen is loaded in a standard three point configuration until failure is observed. When observing a load versus time plot, a sudden drop in load indicates failure. From this, the resulting shear

stress can be calculated and the adhesion strength can be quantified. A disadvantage with this test is aging difficulties due to most of the adhesive layer not being exposed. Also, there is potential for failure within the adhesive itself as opposed to the adhesive-metal interface. Finally, the nature of this test concentrates the maximum moment directly in the center of testing, so that any misalignment of the specimen will results in critical errors [7].

The four point bend test is a modification to the three point bend test. It calls for two load points located outside of the two displacement pins. Unlike the three point bend configuration, the four-point applies a constant moment to the bonded interface (Figure 1-3b). A benefit to this test is it allows for steady state crack propagation when the crack length exceeds the thickness of the upper layer, thus simplifying the analysis. For an advancing crack in this configuration, the energy release rate is independent of crack length, thus leading to a more stable energy release rate calculation. However, the environmental aging and failure mode uncertainties still exist with this model [8].

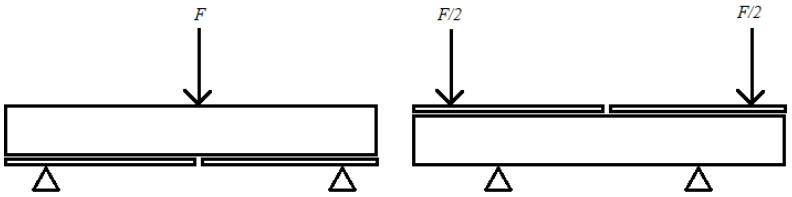

(a) (b)

Figure 1-3. Schematics of three (a) and four (b) point bend tests.

1.4.4 Blister Test

The blister test was developed as an adhesion testing methods ideal for thin flexible membranes on rigid substrates. Thin film layers are very common in electronic packaging applications ranging in application from die attach films to conformal coating layers for tin whisker mitigation. A known thickness of a polymer in question is adhered to the top side of a rigid substrate above a small pressure hole. An increasing pressure load is applied to the underside of the polymer via the pressure hole, thus eventually creating a circular debond (blister) which grows in size. The height of the blister is recorded, providing a pressure and height relationship. Analysis of this relationship in conjunction with the debond radius can allow one to gain insight into the energy release rate of a material. The disadvantages to this approach include difficulty in dynamically measuring the debond radius and inaccuracies when the blister height exceeds a value known as the spherical limit. In addition, this approach assumes a constant Young's modulus for all loading conditions which may not be accurate when considering the rate-dependent modulus of many polymers.

1.4.5 Advanced Blister Test

In the spirit of the standard blister test mentioned in the previous section, this work brings to light a new method, hence forth referred to as the advanced blister test (ABT). The ABT allows for in situ measurement of the polymer modulus for each test which can increase the accuracy of calculations should the modulus be inconsistent under varying loading conditions. In addition, the method takes advantage of revised specimen preparation to introduce a low-adhesion, circular precrack area of radius, *a*, which defines

an initial known blister diameter of constant thickness, *t*. Because this is the case, the experimenter is most interested in understanding the pressure and height at which crack propagation begins within a sample (critical pressure, critical height). This point is determined by monitoring the pressure (*P)* vs. height (*w*) relationship. The energy release rate is then calculated by considering an infinitesimally small crack growth from that point forward. This experiment eliminates the need to dynamically measure the blister diameter which can be seen as a major advantage. However, despite these advancements, every test has its limits. The ABT will not be valid for polymer layers which will undergo large deformations prior to reaching the critical point. A schematic of the ABT can be seen in Figure 1-4.

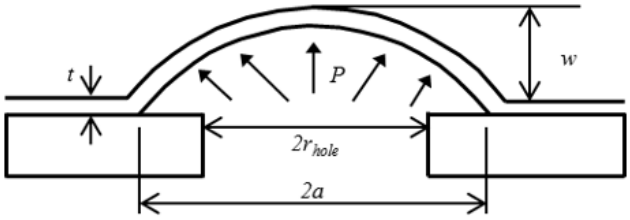

Figure 1-4. Schematic of ABT test setup.

CHAPTER 2: DESCRIPTION OF BLISTER TEST

2.1 Derivation of Stress and Stain in Film Layer

The ABT is remarkably similar to a problem frequently posed in classical engineering – a circular pressurized plate. The boundary conditions for the problem assume a maximum deflection at the center of the blister and that the blister's edges are clamped. Therefore, it is evident that the slope of the blister is zero along the circumference and at the center. Numerically, this is described as the following:

$$\left.\frac{\partial w}{\partial r}\right|_{r=o,a} = 0 \tag{2.1}$$

where w is the deflection, r is the radial distance from the center of the blister, and a is the blister radius. A schematic of the plate is shown in Figure 2-1.

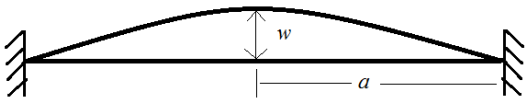

Figure 2-1. Uniformly loaded circular plate with clamped edges.

The pressurized plate can deform via two modes: bending and stretching. A thick and rigid plate would be likely to deform via the stretching mode whereas a thin and flexible membrane would be likely to deform via the stretching mode. We begin by examining each mode individually.

2.1.1 Bending Only Mode

A blister is considered to be in the bending mode when its deflection is much smaller than its thickness. For the bending case, Timoshenko [9] derives the slope of a uniformly circular plate to be:

$$\frac{\partial w}{\partial r} = \frac{qr^3}{16D} + \frac{C_1 r}{2} + \frac{C_2}{r} \tag{2.2}$$

where C_1 and C_2 are constants and D is the flexural rigidity of the plate:

$$D = \frac{Et^3}{12(1-\upsilon^2)} \tag{2.3}$$

where υ is the Poisson's ratio of the material and *E* is the Young's modulus. Considering the boundary conditions, the following relationship for pressure and height can be derived:

$$w_{\max} = \frac{3Pa^4(1-\upsilon^2)}{16Et^3} \tag{2.4}$$

$$P = \frac{16Et^3 w}{3a^4(1-\upsilon^2)} \tag{2.5}$$

where υ is the Poisson's ratio of the material and *E* is the Young's modulus. The stress at the center of the blister can now be solved:

$$M(0) = \frac{Pa^2(1+\nu)}{16} \tag{2.6}$$

$$\sigma(0) = \frac{6}{t^2} M(0) \tag{2.7}$$

$$\sigma = \frac{3(1+\nu)Pa^2}{8t^2} \tag{2.8}$$

Using a linear elastic constitutive relationship, the strain can be determined as well:

$$\varepsilon = \frac{1}{E}\left(\sigma_\theta - \nu\sigma_\psi\right) \tag{2.9}$$

which leads to:

$$\varepsilon = \frac{2tw}{a^2} \tag{2.10}$$

2.1.2: Stretching Only Mode

This stretching mode occurs when the blister's deflection is much greater than its thickness. Analysis of this mode relies on several key assumptions to determine the stress-strain relationship. First, the deflection of the blister is assumed to take the shape of a spherical cap of radius *R*. When the blister deflection is very small, $w << a$, the radius can be approximated as the following:

$$R = \frac{a^2 + w^2}{2w} \approx \frac{a^2}{2w} \tag{2.11}$$

The strain can now be ascertained from the geometric relationship:

$$\varepsilon = \frac{2\left(\frac{w}{a}\right)^2}{3\left(\left(\frac{w}{a}\right)^2 + 1\right)^2} \approx \frac{2}{3}\left(\frac{w}{a}\right)^2 \tag{2.12}$$

Another assumption made is that the thin film layer is a thin elastic membrane and that there are no changes in stress throughout the thickness. With this assumption the meridional and circumferential stresses in the layer are identical and the same as a thin-walled pressure vessel. Consequently, the stress in the film can be approximated as the following:

$$\sigma = \frac{PR}{2t} = \frac{P(a^2 + w^2)}{4wt} \approx \frac{Pa^2}{4wt} \tag{2.13}$$

Considering a linear elastic constitutive relationship between stress and strain, the following relationships between pressure and blister height can be defined [10, 11]:

$$w = \left[\frac{3Pa^4(1-\upsilon)}{8Et} \right]^{\frac{1}{3}} \tag{2.14}$$

$$P = \frac{8w^3Et}{3a^4(1-\upsilon)} \tag{2.15}$$

For a more practical interpretation of the very small deflection assumption, the percent error between the true and assumed strain values in plotted in Figure 2-2. As can be seen, the error in strain is less than 2% when the blister radius is at least 10 times larger than the critical blister height. Therefore, it is important that experiments are designed in such a way that the blister will not deflect beyond this limit before delamination to preserve accuracy. The resulting testing criterion for the small deflections assumption to be valid is:

$$\frac{a}{w} > 10 \tag{2.16}$$

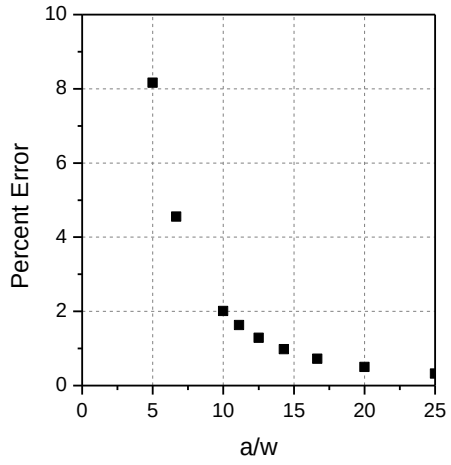

Figure 2-2. Percent error in strain vs normalized blister radii with blister height.

2.2 Determination of the Energy Release Rate through the Energy Balance Method

To evaluate the energy release rate, G, an energy balance method is employed at the critical moment the blister delaminates. At this state, the critical pressure, P_{crit}, is assumed to be constant and two cases are examined: the moment before delamination when the blister radius is still a, and the moment after an infinitesimal delamination of Δa when the blister radius is $a + \Delta a$. The energy balance we are interested in is the difference between these two key states at constant pressure, P_{crit}:

$$\Delta W = \Delta W_1 + \Delta W_2 \tag{2.17}$$

where the change in work input into the system, ΔW, is evaluated as:

$$\Delta W = P_{Crit}\Delta V = P_{Crit}\left(V\big|_{a+\Delta a} - V\big|_a\right) \tag{2.18}$$

where V is the volume of the blister. The energy dissipated when the crack propagates, ΔW_1, is evaluated as:

$$\Delta W_1 = 2\pi G \Delta a \tag{2.19}$$

and the change in energy stored in the film layer, ΔW_2, is evaluated as:

$$\Delta W_2 = \int \sigma d\varepsilon\Big|_{a+\Delta a} - \int \sigma d\varepsilon\Big|_a \tag{2.20}$$

Combining Equations (2.18), (2.19), and (2.20) into (2.17) the energy release rate can be expressed as:

$$G = \left(\frac{P_{crit}(V\,|_{a+\Delta a} - V_a) - \left(W_{2_{a+\Delta a}} - W_{2_a}\right)}{2\pi a \Delta a} \right) \tag{2.21}$$

Expressions for G can be determined analytically for either bending only or stretching only cases. Both ideal cases will be now be investigated.

2.2.1 Determination of Energy Release Rate: Bending Only Case

By integrating the blister height as a function of radial position of the blister, the blister volume can be directly evaluated:

$$V = 2\pi \int_0^a w(r) r dr \tag{2.22}$$

The change in work input at the critical state for an infinitesimal crack extension of Δa can then be expressed as:

$$\Delta W = 2\pi \int_0^a P_{Crit} \Delta a w(r) r dr \tag{2.23}$$

The energy stored in the film simplifies to [12]:

$$W_2 = \int \sigma d\varepsilon = \left(\frac{PV}{2} \right) \tag{2.24}$$

Such that the change in energy stored in the film becomes:

$$\Delta W_2 = \frac{1}{2} \Delta W \tag{2.25}$$

Combining Equations (2.22), (2.23), (2.25) into (2.17) and rearranging, it can be found that the energy release rate for the bending only case can be expressed as:

$$G = \frac{3\left(1-\nu^2\right)a^4}{32Et^3} \cdot P_{Crit}^2 \tag{2.26}$$

2.2.2 Determination of Energy Release Rate: Stretching Only Case

In his work, Gent [11] explains the numerical derivation of energy release rate for the stretching case. First, the blister volume is evaluated by once again considering a blister with a spherical cap:

$$V = C_1 \pi a^2 w \tag{2.27}$$

where C_1 is a numerical constant to accommodate the volume difference of the spherical cap due to the clamped end condition of the blister. For a typical polymer Poisson's ratio $C_1 = 0.518$ has been reported in the literature [11, 13]. The amount of work inputted into the system is related to the incremental change in volume with constant pressure as the circular debond area extends by a differential amount, Δa. Expressed mathematically:

$$\Delta W = P\left(\frac{\partial V}{\partial a}\right)\Delta a = \left(\frac{10PV}{3a}\right)\Delta a \tag{2.28}$$

Also, the amount of energy stored in the membrane can be simply expressed as:

$$W_2 = \left(\frac{PV}{4}\right) \tag{2.29}$$

So that

$$\Delta W_2 = \frac{\Delta W}{4} \tag{2.30}$$

Combining Equations (2.27)-(2.30) into Equation (2.17) the energy release rate for the stretching only model can be expressed:

$$G = \left[\frac{5}{4}\left(\frac{3}{8}\right)^{1/3}\right] C_1 \left(\frac{P_{Crit}^4 a^4 (1-\nu)}{Et}\right)^{\frac{1}{3}} \tag{2.31}$$

2.3 Blister Testing of Real Samples

For the case of the ideal ABT test, specimens deform by neither via pure bending or pure stretching. In fact, they deform via both modes simultaneously. When testing a flexible polymer layer using the ABT, it is not initially clear whether the blister deformation mode will be bending or stretching dominant. First, the dependence can be visually inspected by plotting the numerical equations against the experimental results. Equations (2.4) and (2.15) representing the bending and stretching cases respectively, and experimental data are plotted in Figure 2-3 below. For all three cases, a radius of 4.7625 mm, a thickness of 0.311 mm, Poisson's ratio of 0.4, and modulus of 2.70 GPa were used. These parameters were selected based off of the configuration for the experimental case. After plotting, it is evident that the experimental data falls in between the bending and stretching modes suggesting deformation via both modes.

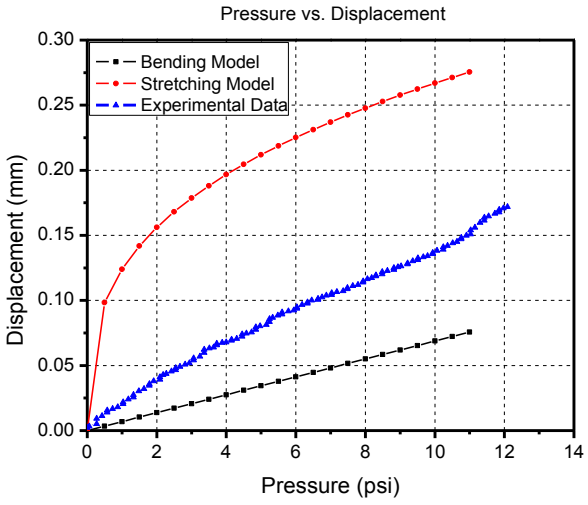

Figure 2-3. Typical displacement versus pressure blister test results compared to ideal cases.

Because of the lack of an analytical description to how the bending and stretching modes will interact in an experiment, FEM modeling software can be taken advantage of to predict the behavior of a specimen. After conducting an experiment, a nonlinear regression analysis using the FEM model can be run iteratively until the pressure versus displacement curve best matches the experimental data. Once the corresponding set of parameters is extracted from the resulting model, the modulus of the specimen is reported. Due to uncertainties with the rate-dependency of the modulus characterization, this process is repeated for each test to ensure accuracy.

Once the modulus is calculated, the energy release rate can be found through FEA and Matlab calculations. FEA tools such as ANSYS are readily available and allow for cases to be examined when the case does not fall under some ideal analytical expression. Instead, the formulation seen in Equation (2.21) can be used directly to evaluate G. By running the model iteratively at several radius values (each increasing by Δa), the relevant parameters can be extracted from the model to determine the energy release rate in each case. Using a linear fit, the energy release rate can then be determined as Δa approaches zero, thus allowing for an accurate determination of the energy release rate.

CHAPTER 3: SAMPLE PREPARATION

3.1 Motivation

The motivation behind the sample preparation is to develop a simple to follow method to create well-defined advanced blister test specimens without the use of specialized equipment. The radius dependency of the adhesion strength is obviously seen in both bending only Equation (2.26) and stretching only Equation (2.31) cases. To minimize errors from the blister radius, a circular, well-defined predefined area is required. Small deviations to the circular blister area can yield unwanted stress concentrations and lead to errors in adhesion strength calculation. In addition, the area should ideally have extremely low adhesion so that a small pressure load will define the initial blister radius, reducing the possibility for damage before delamination beyond the predefined area. Finally, the blister layer should be flat, smooth, and uniform among each sample so that the measured thickness values are accurate.

The sample preparation used in this work takes advantage of a copper substrate and Hysol F114 tra-bond epoxy. The copper substrate was chosen for its rigidity, ensuring that all work energy is transferred to the blister itself. F114 epoxy was chosen due to its low viscosity, fast curing time, and flexible properties. It was also hypothesized that the F114 material will not undergo any significant plastic deformations prior to failure and will deform elastically throughout the experiment. The experiment can be extended to many rigid substrate and linear membrane combinations.

3.2 Fabrication

The blister substrates are prepared using general purpose copper with twelve evenly-spaced 0.15” pressure holes, seen below in Figure 3-1

Figure 3-1. Copper substrate for blister test samples.

Each copper substrate is subjected to successive grinding using a rotational grinding machine set at 150 RPM. The substrates are grinded using 240, 400, 600, and 800 grit paper for five minutes each. This process helps ensure a uniform surface roughness on order of ~6.5 μm while removing any impurities that may have been introduced by previous experimental procedures. After grinding, the substrates are washed using distilled water and then wiped using methanol for further cleaning.

A stencil piece composed of flat sheet metal with 12 3/8” diameter holes is placed on top of the substrate so that the stencil holes are concentric with the pressure holes. Using scotch tape, the stencil piece is taped along its edges to the substrate, seen in Figure 3-2. The exposed substrate areas will be the predefined areas for 12 blisters.

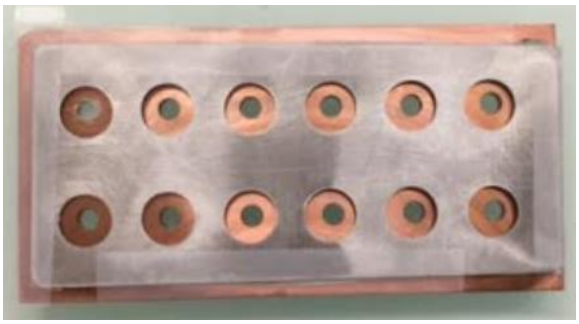

Figure 3-2. Copper substrate with attached stencil.

Pieces of scotch tape are applied to the substrates to contact the newly defined predefined areas and pressed using a wooden stick. By avoiding tape contact outside the predefined area by use of the stencil, the possibility of introducing impurities to the region of interest is greatly reduced. This system is seen in Figure 3-3. The substrate and stencil system is then turned upside-down so that the exposed ends of the pressure holes are face up.

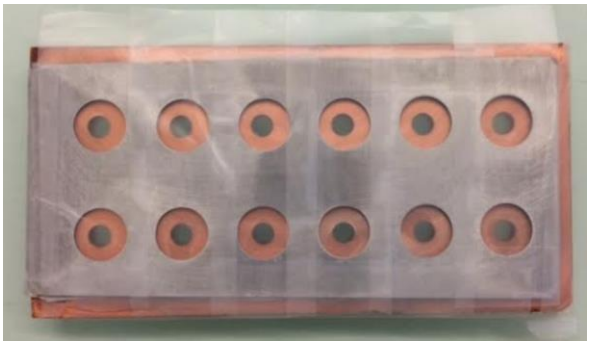

Figure 3-3. Copper substrate with attached stencil and predefined area seal.

Two grams per substrate of GE Silicon Compound RTV615A is prepared according to the manufacturer's specification and then spun in a centrifuge for 3-5 minutes to remove any gas introduced by mixing. The compound is then carefully poured into each pressure hole, ensuring no gas bubbles form in the process. Meanwhile, 12 1.5 millimeter

diameter dowel pins are allowed to soak in GE SS4120 primer for five minutes, then allowed to dry for five minutes. By doing so, the dowel pins will be able to adhere to silicon rubber. A pin is carefully inserted into each pressure hole, serving as a convenient way to remove the silicon plugs later in the process. The system is allowed to cure for 24 hours at room temperature. Silicon rubber was chosen for its known low adhesion properties which will ensure that it will not adhere to the scotch tape, blister material, or copper.

After a full cure, the tape covering the end of each pressure hole is carefully removed with the help of applying a small amount of methanol to the top surface of each tape. The stencil is then removed and the entire substrate is once again wiped with methanol to reduce the possibility of contamination from the tape's adhesive material. After securing the stencil again, two sprays of Sprayon MR311 dry film release agent are applied, thus defining a low adhesion predefined area for each blister specimen. The use of a wet release agent, such as silicon oil, proved to be unsuccessful due to transport and mixing issues with the blister material.

An 18" length of 0.01" diameter 99.99% pure aluminum wire is then deposited on top of the dry film release agent via the use of a Denton DV-502A vacuum chamber. The release agent and aluminum layers compose the completed predefined area.
A reservoir for the blister material is created using known thicknesses of scotch tape (0.060" thick). For the ideal test, about five layers of scotch tape were used, thus defining a depth of about 0.300". The tape must be applied in such a way that it is fully

secured and there are no gaps from which epoxy may leak. The substrate is then placed on a surface known to be completely leveled.

Next, Hysol F114 tra-bond epoxy is prepared. The two part system is mixed and spun in the centrifuge for roughly two minutes. Since the working time for the material is only about 10 minutes, it is important to work quickly. After preparation, the F114 is poured into the reservoir and allowed to spread via gravity with the assistance of a wooden stick. It is not crucial for the F114 thickness to match the reservoir thickness perfectly as each blister thickness will be measured and accounted for in subsequent steps. Next, the F114 is allowed to cure at room temperature for 48 hours. After the full cure is achieved, the silicon plugs may be removed by pulling the dowel pins. The plugs should easily be removed from the system with no adhesion to the F114 or copper substrate. Finally, the cured F114 is cut into twelve distinct sections, each containing a predefined area, using a small blade. This ensures that delamination from one sample will not affect the others during testing.

3.3 Environmental Conditioning

In addition to the specimen preparation procedures outlined above, additional steps can be taken to subject the blister specimens to environmental conditioning. Environmental factors such as moisture content and thermal aging can significantly affect the adhesion strength after long term exposure. Later in this work, degradation related to moisture exposure for seven days is investigated and reported. Additionally, the effect of thermal aging near and far above the glass transition temperature is investigated and reported.

CHAPTER 4: EXPERIMENTAL SETUP, PROCEDURE, AND DATA

4.1 Motivation

The required test setup for the advanced blister test requires the capture and live synthesis of blister pressure and height data from separate instruments. Doing so allows the experimenter to view data in such a way that blister delamination will be evident via slope change in the plot. In addition, the data should be stored in such a way that it is easy to post process using FEM software. In addition, video of each test will be captured both for verification purposes of delamination and for future reference. The setup must be constructed in such a way that it is stable and produces repeatable results, thus not introducing unwanted unknowns into the problem.

4.2 Overview of Experimental Setup

To capture all the required data, an integrated LabView program was created to synchronize data collection from three separate sources, namely, a Tescom ER3000 pressure regulator, a MTI MicroTrak II laser displacement sensor, and a Sentech MC133-USB camera. A schematic and photograph of the experimental setup can be seen below in Figure 4-1 and Figure 4-2, respectively.

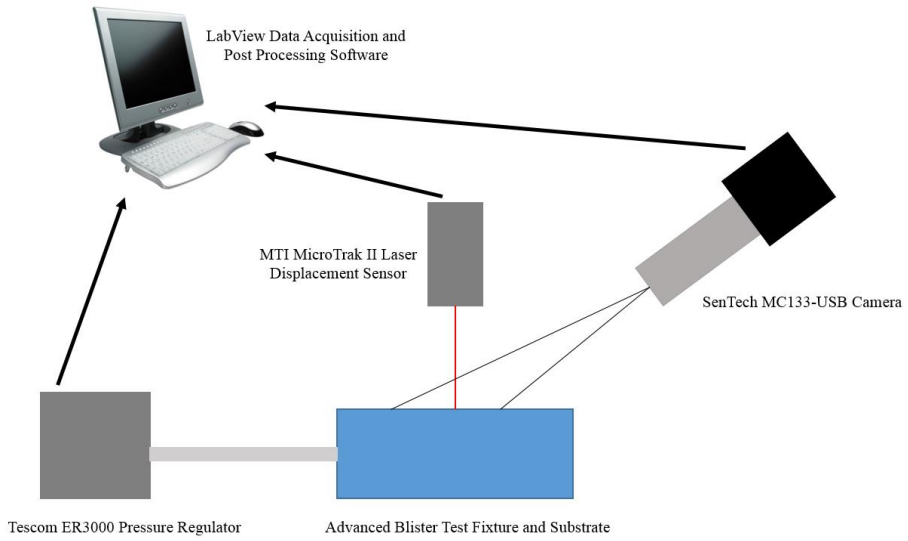

Figure 4-1. Schematic of experimental setup.

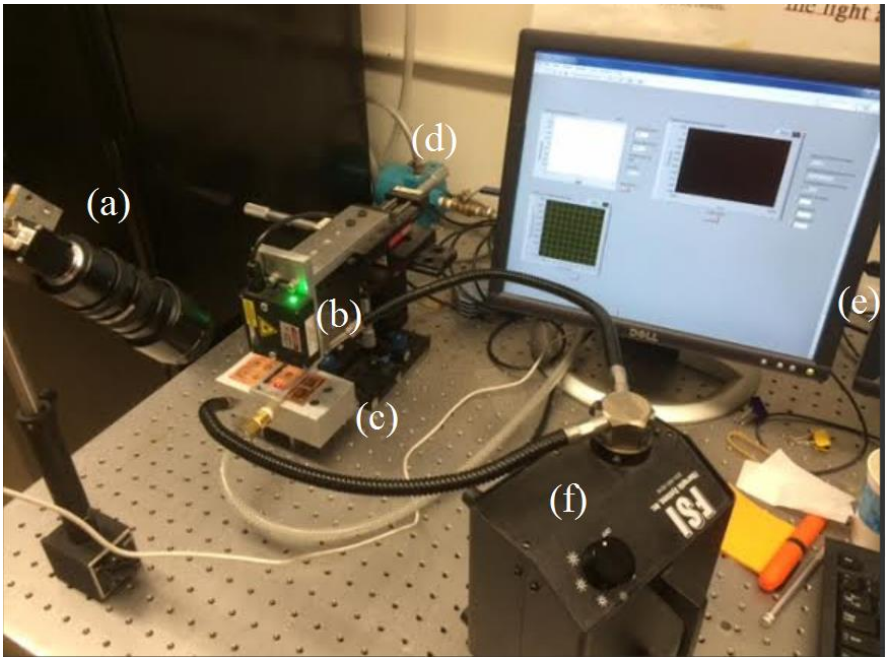

Figure 4-2. Photograph of experimental setup showing: (a) USB camera (b) laser displacement sensor (c) specimen fixture with substrate (d) pressure regulator (e) LabView module (f) optional light source

The Advanced Blister Test fixture consists of a custom machined aluminum base with a pressure inlet, o-ring gaskets, and a screw clamp. The gaskets provide a pressure seal when used in combination with Dow Corning high vacuum grease. The screw clamp provides pressure along the edges of a blister specimen to ensure snug contact with the gaskets. In addition, it has an open top face to allow for vertical deformation as well as visual inspection. This setup was specifically crafted for the aluminum substrates described in section 3.1. The fixture also has four ¼-20 bolt through holes to rigidly mount it to an appropriate table. A photograph of the fixture can be seen below in Figure 4-3.

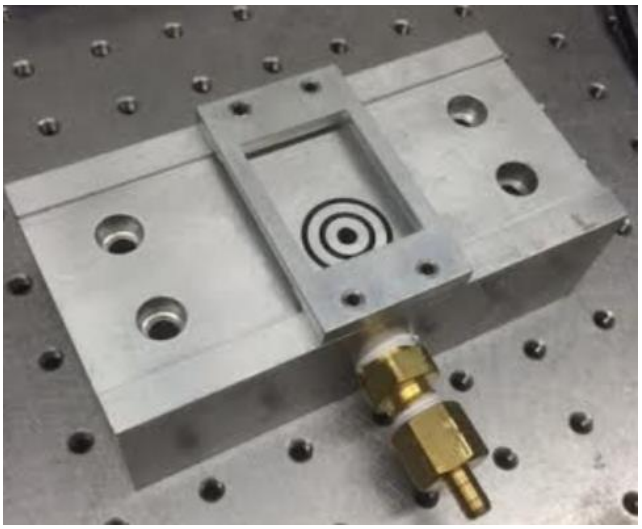

Figure 4-3. Advanced blister test fixture.

According to the manufacturer's specifications, the MicroTrak II laser displacement sensor is capable of a resolution of 1.25 micrometers and is therefore very sensitive to small movements or vibrations. Because of this, a rigid mount was designed specifically for the instrument. The mount positioning is controlled by a three-axis translation stage.

This ensures accurate alignment of the laser above the blister specimen's geometric center so that the maximum deflection is captured in each test.

The Tescom ER3000 pressure regulator is rigidly mounted to the experiment table and attached to the pressure inlet of the fixture's pressure inlet through the use of standard tubing. The system is routinely checked for possible leaks.

The SenTech MC133-USB camera is mounted to a vertical stand behind the fixture using built-in mounting features. A Zoom 100 lens is used in conjunction with the camera due to its ability to capture the entire field of view. The camera and lens setup is angled so that the entire blister sample being tested is visible. Because of the angle, the circular blister becomes slightly distorted. However since the proposed experimental procedure does not involve image post-processing for calculations, a slightly distorted video is acceptable. In addition, a high power light source is optionally used to help wash out the red spot introduced by the laser displacement sensor. By doing so, a clearer video may be easily obtained. It is important to note that captured video is only used for data verification and visual inspection purposes.

4.3 LabView Module

The LabView module developed for the advanced blister test combines the functionality of all the equipment into one easy to use package. Although each device has its own stand-alone software package provided by the manufacturer, it is difficult and tedious to individual capture and synchronize pressure and displacement data. The module controls

each piece of equipment and allows the operator to control some of the input variables before testing. The program is optimized on a computer system with two monitors so that a large image may be viewed. A screenshot of the module may be seen below in Figure 4-4. Screen captured image of LabView data capture module. and Figure 4-5. Screen captured image of LabView image capture module.

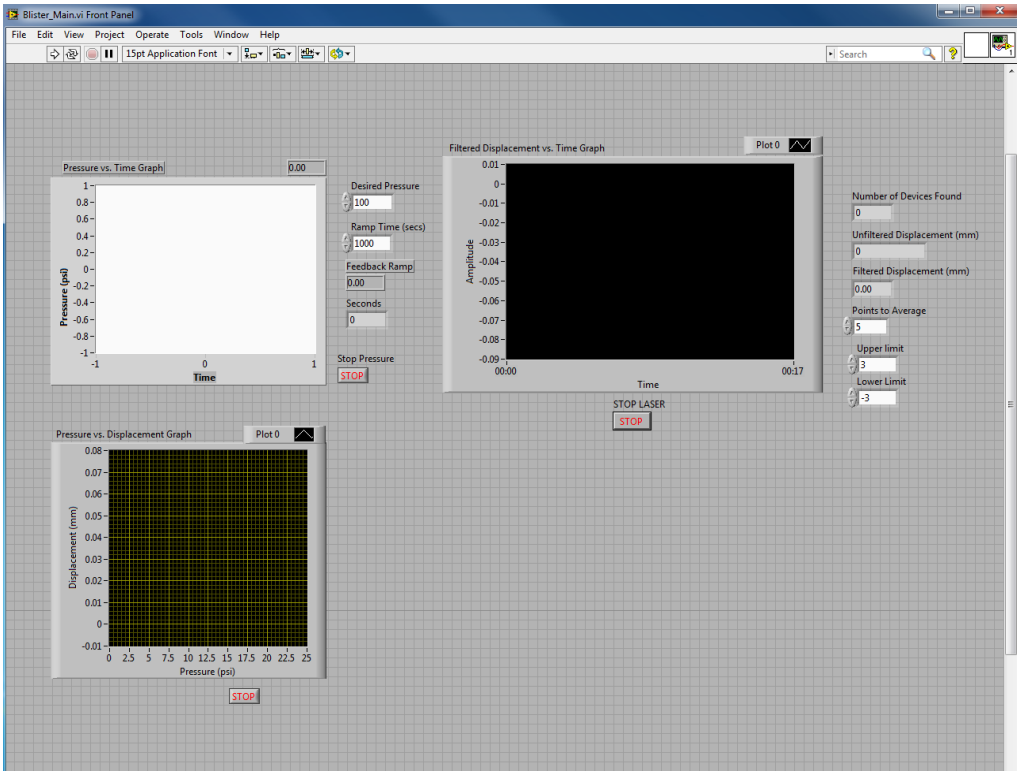

Figure 4-4. Screen captured image of LabView data capture module.

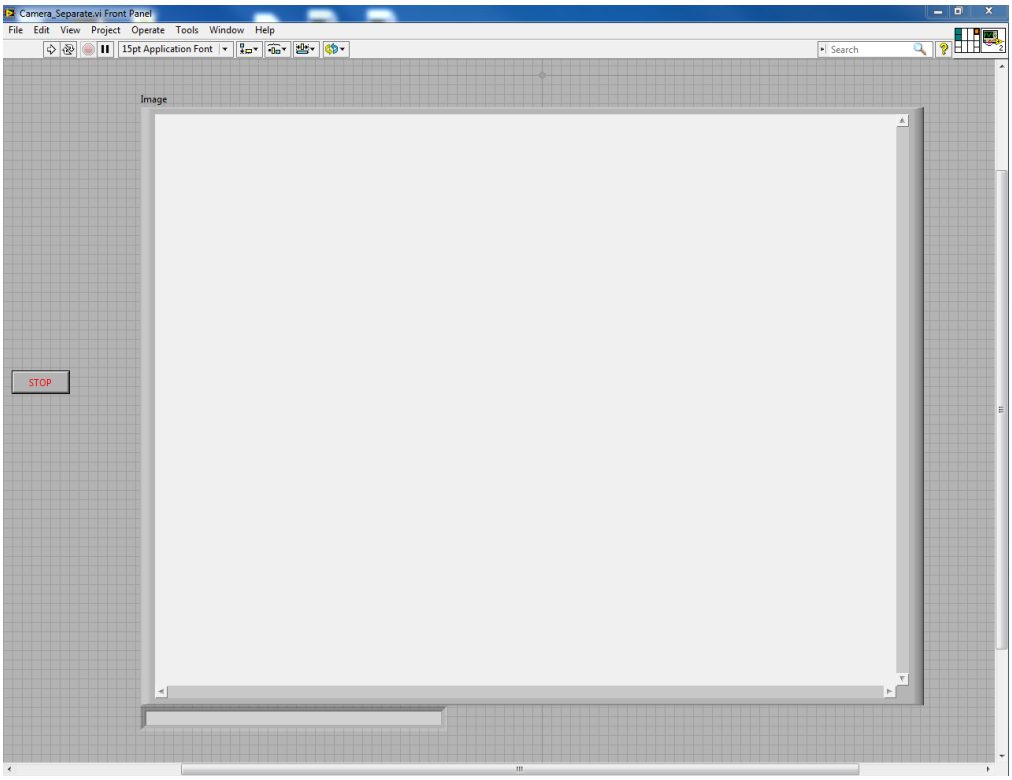

Figure 4-5. Screen captured image of LabView image capture module.

Before running the program, the operator must set the values of five variables, two related to the pressure regulator and three related to the laser displacement sensor. The "desired pressure" field indicates the maximum pressure in psi that the regulator should output. The "ramp time" field indicates the amount of time in which the pressure regulator should take to achieve the "desired pressure" indicated. The regulator linearly increases its pressure to the "desired pressure" in the "ramp time", thus defining a ramp profile. If at any point during the experiment the ramp needs to be stopped, the corresponding stop button will terminate the ramp by stepping the pressure to 0 psi. If the ramp is not stopped before the "desired pressure" is reached, the regulator will hold this value until the user stops the program, at which time the regulator pressure will step to zero psi. The "feedback ramp" field indicates the pressure the regulator is reading.

The “seconds” field indicates the time passed, in seconds, since the start of the ramp profile. The “pressure vs. time graph” outputs a live feed of time, in seconds, versus pressure read, in psi.

The laser displacement sensor outputs very noisy data unless it is filtered in such a way that the data is useful. A boxcar averaging technique is used to smooth the data, thus reducing the influence of small spikes in the data from point to point. A small number of adjacent points are averaged together and read as a single point. The “points to average” field allows the user to select the number of points to include in each calculation. A default value of five has shown to work well for this application. An upper and lower limit may also be set via their respective fields. If the displacement sensor reads a value, in millimeters, either larger than the upper limit or smaller than the lower limit, it will output a value of zero. This will help remove large spikes in the data. Other filtering techniques used in addition to these methods will be discussed in a later chapter. The “number of devices found” field indicates whether the system is able to properly communicate with the laser displacement sensor, which is a way to verify the system is working properly. The “unfiltered displacement” field shows a live feed of the raw data read by the sensor and the “filtered displacement” field shows a live feed of the data after being processed by the filters. The corresponding “stop” button stops the laser displacement sensor from collecting data. The “filtered displacement vs. time” graph outputs a live feed of time, in seconds, versus displacement, in millimeters.

At a constant interval of every 0.1 seconds, the values read by the pressure regulator and laser displacement sensor (after filtering), are collected and graphed against each other in

the “pressure vs. displacement graph” window. The data may be saved as an excel spreadsheet simply by right clicking on the graph itself and selecting the appropriate option. The stop button below this graph stops the process of collecting and graphing the data. In addition, when the program is started it launches a separate module that automatically captures live video from the experiment. When the user presses the corresponding stop button or when the entire program is stopped, the module automatically saves the video to the user’s desktop in .avi format.

4.4 Experimental Procedure

After ensuring proper setup of the equipment, an advanced blister test is ready to be run. The thickness of each blister specimen is measured by using a Mitutoyo micrometer with 0.001 mm resolution. By subtracting the thickness of the substrate from the measured thickness of the substrate and F114 layer, it is simple to obtain the thickness value for each blister.

Before placing a specimen into the fixture, the underside of the blister is lightly pressed upon with a wooden stick to promote a small amount of delamination within the predefined area. Doing so ensures there is no adhesion between the F114 and edges of the pressure hole. Pressing too hard may cause undesired delamination outside of the predefined area, rendering the sample unusable.

Next, a small amount of Dow Corning high vacuum grease is applied to the o-ring gaskets and the specimen is properly aligned within the fixture. The cover piece is

securely attached by the use of four screws along its perimeter. The laser displacement sensor is then turned on and visually aligned with the x and y direction translational stages so that the measured area is in the center of the blister being tested. After ensuring proper alignment, the laser displacement sensor is then "zeroed" by adjusting the z direction translational stage. Finally, the pressure regulator and camera are turned on and the experiment is ready to begin.

For each blister specimen, two iterations of the LabView module are needed. The first iteration loads the blister at a slow rate until the predefined area is fully delaminated. A slow rate is chosen so that accidental delamination beyond the predefined area by excessive loading is avoided. By setting the rate at 0.1 psi per second and running the module, the pressure vs. displacement graph and video output are observed. A gradual change in slope followed by stability will be seen, indicating separation. The video feed should be cross referenced to determine whether the separation can be visually confirmed. Examples of this initial data can be seen below in Figure 4-6.

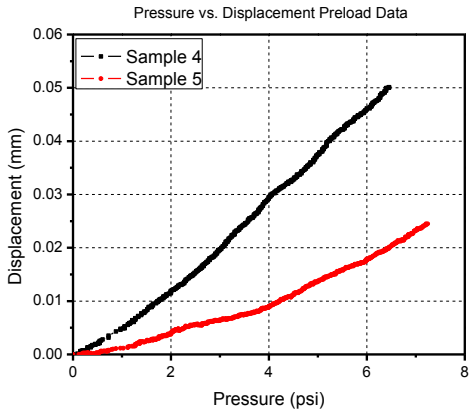

Figure 4-6. Typical displacement versus load graph of blister test.

The second iteration of the program involves increasing the pressure at a much faster rate, 1 psi per second. The blister is loaded until clear delamination beyond the predefined area occurs. Looking at the pressure vs. displacement graph either a jump or an obvious change of slope will be seen at a specific point. The point where this is observed is recorded and will be referred to as the critical point for the experiment. The faster rate is chosen for the test so that the data may show an obvious critical point. A rate faster than 1 psi per second is not practical since the blister will likely fail very quickly making it difficult to cross reference the captured video. Photographs of a blister before and after delamination can be seen below in Figure 4-7.

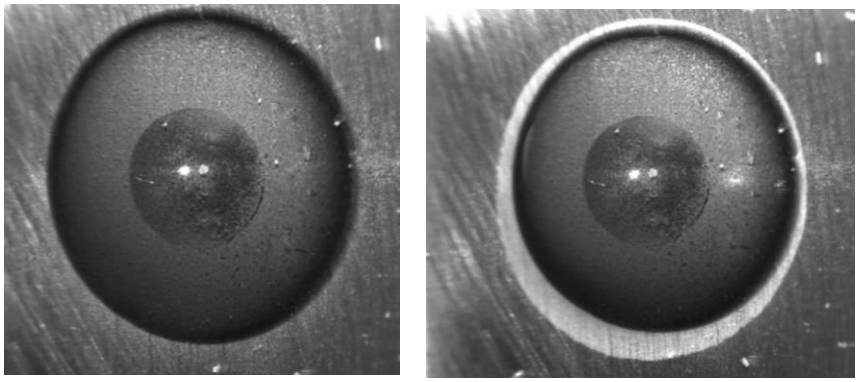

(a) (b)

Figure 4-7 Blister specimen (a) before delamination and (b) after delamination

Twelve specimens were analyzed for this experiment. The measured specimen properties: thicknesses, critical pressures, and critical heights can be seen in Table 4-1, and the corresponding displacement versus pressure curves can be seen in Figure 4-8**.**

Table 4-1. Raw data for as-is test specimen.

Sample	Thickness (mm)	Critical Pressure (psi)	Critical Height (mm)
1	0.240	11.97	0.143
2	0.343	17.67	0.104
3	0.282	16.39	0.162
4	0.311	16.64	0.119
5	0.365	22.27	0.098
6	0.351	23.09	0.107
7	0.307	15.91	0.087
8	0.310	17.91	0.104
9	0.265	18.20	0.085
10	0.312	24.90	0.084
11	0.295	17.80	0.115
12	0.335	24.60	0.078

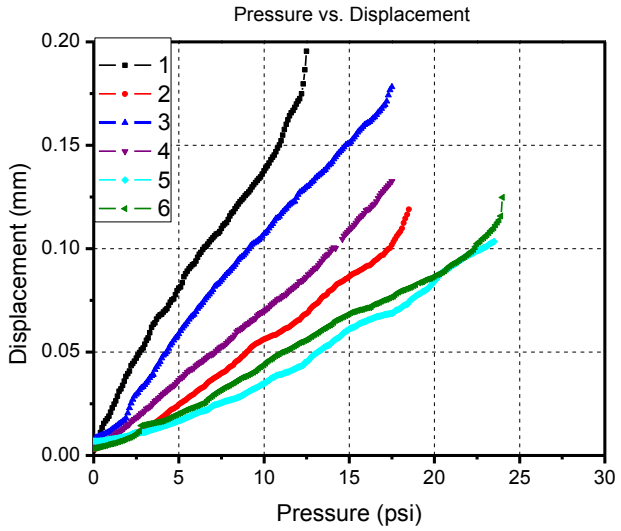

(a)

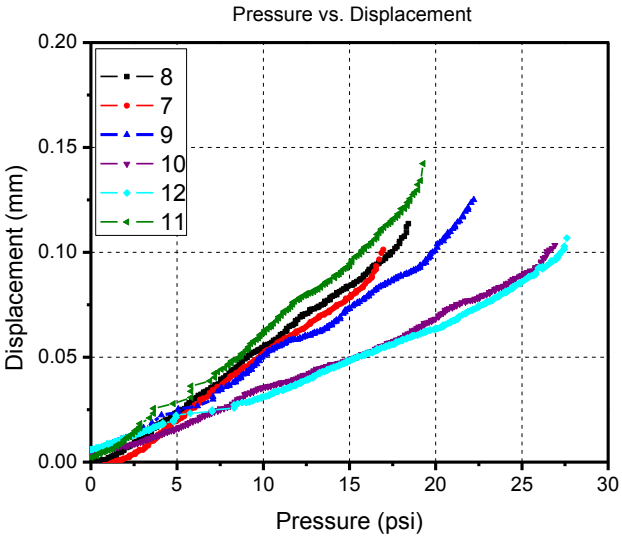

(b)

Figure 4-8. As-is specimen displacement versus pressure curves for samples (a) 1-6, and (b) 7-12.

CHAPTER 5: DETERMINATION OF PSEUDO-MODULUS AND ADHESION STRENGTH USING FEA

5.1 Data Preparation

Before calculating the modulus and energy release rate of each specimen, the raw data must be carefully processed in such a way that accurate and consistent results are obtained. Due to the nature of the experiment, the pressure reading often does not increase at a perfectly linear rate as the blister deforms. This is hypothesized to be attributed to small plastic deformations and small inaccuracies within the pressure regulator setup. In addition, the data collected may have collected duplicate displacement measurements for a given pressure. Although the pressure regulator is set to a ramp profile, it in fact achieves this profile via small and evenly space steps. It is sometimes the case that two data points are collected at a single step since data is recorded at a fast rate. Because of this, these reasons, the spacing of data points along the x direction may not be evenly spaced, or there may be duplicates.

Also, it is evident that during an advanced blister test, the early data do not appear to follow a linear trend. This is due to small plastic deformations in the sample caused by the initial loading used to separate the predefined area. The deformations caused by plastic deformation can be found by examining the height of the blister at 0 psi. Since the deformations only range from roughly 3-6 micrometers, the effect can be considered negligible when considering the accuracy of results. For almost all tests conducted, the

data follow this random pattern before 2 psi loading. By removing data from 3 psi and before, the influence is removed for all cases. In addition, all data beyond the critical pressure is removed as well since it will not be used in calculation.

To resolve these issues, three Excel functions were created. The first averages duplicate height values when a pressure value is repeated so that each pressure value is unique. The second "steps" the data at 0.1 psi pressure intervals. This is done through linear interpolation of neighboring pressure values. The third laterally "shifts" the data so that the line of best fit for data set passes through the origin. In a theoretical sense, a loading of 0 psi should correspond to 0 deformation.

5.2 Using FEM and Matlab to Solve for Pseudo-Modulus

FEM is used in conjunction with Matlab to solve for the modulus value in each data set. The thickness, Poisson's ratio, critical pressure, processed data, and modulus are all inputs into the program. A Poisson's ratio of 0.4 is assumed for every sample. Since the problem is of an axisymmetric nature, the model is relatively simple and quick to run. A constant geometry for the substrate thickness, substrate length, substrate material properties, and predefined area radius are used since this remains the same between all tests. A PLANE183 2 dimensional structural brick element is used for the mesh in the model. The element has eight modes and is of serendipity type.

After defining the maximum pressure input to the bottom of the blister, the model is run. The maximum pressure is achieved through the use of a ramp function, recording the

pressure and height data at a finite number of points. The results are then saved into a text file which is used as an input to the Matlab script.

The Matlab script allows the user to input a lower bound, upper bound, and step size for the modulus. These bounds should be based off of an educated guess, or in relation to previous results. The script iteratively runs the ANSYS model varying the modulus value within the defined range, collects the result, and compares it to the experimental data. Each run, the modulus increases by the step size value and a regression analysis is used to judge the fit of the numerical data to experimental data. The r^2 parameter is used as a measure of fit, and the modulus value is used from the numerical data with the best fit. An example of the numerical fit taken from the Matlab output can be seen below in Figure 5-1**.**

Errors in estimating the Possion's ratio can result in modulus calculations with up to a 13% error. Because of this, the FEM calculated modulus is referred to as the pseudo-modulus. It is important to note that this error, however, does not result in any additional error when calculating the energy release rate. This topic is explored further in the discussion section of this thesis.

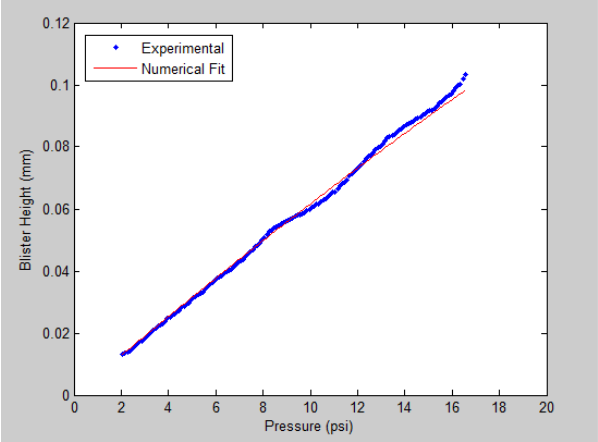

Figure 5-1. Example of numerical fit against experimental data.

5.3 Using FEM to Solve for Energy Release Rate

The general equation for energy release rate can be readily solved by the program. Similar to before, an ANSYS model is run so that the height profile of the blister is obtained at the critical pressure. Instead of recording only the maximum height, however, the entire profile of the blister is obtained and stored in discrete intervals. From this, the three-dimensional trapezoidal method is applied using matlab to obtain the blister volume at a given radius and this value is stored. The strain energy is also calculated is also calculated in each element directly from FEM. The total strain energy is obtained by summing the individual element strain energy and multiplying by 2 pi. This process is repeated for three more times, each increasing the radial dimension by an amount Δa. After obtaining the required data, the G values are calculated for each independent radius value. A polynomial is fit to the points and the corresponding G value at a radius of size a is recorded, this corresponds to the point right before delamination. This value of G is the energy release rate for the sample.

5.4 Results

The results from the FEM and Matlab analysis can be seen below in Table 5-1 Results after analysis

Table 5-1 Results after analysis.

Sample	**Thickness (mm)**	**Critical Pressure (psi)**	**Critical Height (mm)**	**Calculated Pseudo-E (GPa)**	**Calculated G (J/m^2)**
1	0.240	11.97	0.143	3.10	22.08
2	0.343	17.67	0.104	2.85	29.89
3	0.282	16.39	0.162	2.25	35.64
4	0.311	16.64	0.119	2.70	29.75
5	0.365	22.27	0.098	2.75	36.71
6	0.351	23.09	0.107	3.10	38.47
7	0.307	15.91	0.087	3.45	23.84
8	0.310	17.91	0.104	3.25	29.90
9	0.265	18.20	0.085	5.90	26.50
10	0.312	24.90	0.084	5.40	36.20
11	0.295	17.80	0.115	3.20	32.17
12	0.335	24.60	0.078	5.00	32.62

CHAPTER 6: EFFECT OF ENVIRONMENTAL AGING

6.1 Sample Preparation

Sets of samples were placed into a 125 °C chamber for seven days to explore the effect of thermal aging on the adhesion strength of epoxy material. The glass transition temperature of the F114 epoxy is 53 °C. After aging above this temperature, the material was hypothesized to behave differently under identical loading conditions. An industry-standard temperature of 125 °C was chosen so that the effects of thermal aging may be accelerated. Other than the aging, the sample preparation for these specimens was identical to that described in Chapter 3. After removal from the chamber, it is immediately evident that a physical change occurred within the epoxy material. The color of the blister layer changed from clear to a dark yellow color. This can be observed in Figure 6-1 below:

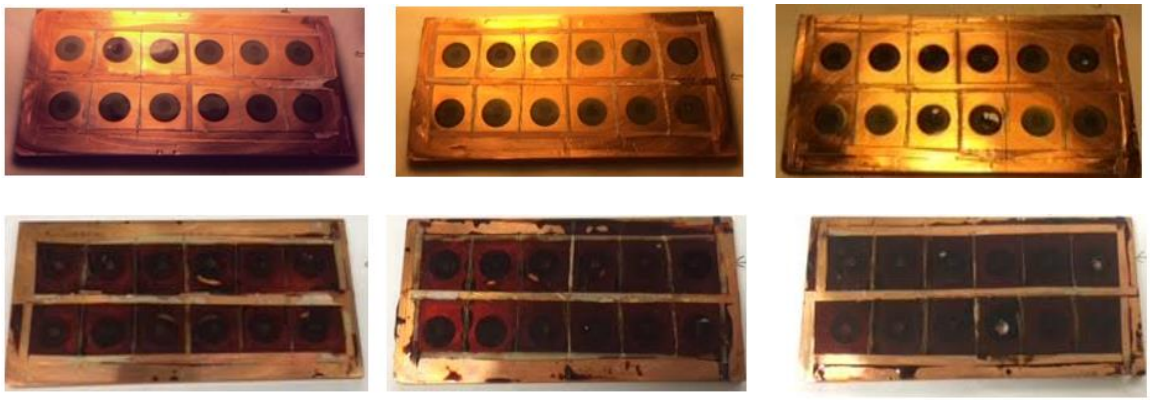

(a) (b) (c)

Figure 6-1. Change in blister appearance after thermal aging. (a)-(c) represent three different sample sets

Alternate sets of samples were placed into a 100% relative humidity chamber for a duration of seven days. The chamber was constructed using a glass container filled with a two inch height of water. Two wooden platforms were created to suspend the samples above the water. The container was sealed using both plastic wrap and aluminum foil. A photograph of the chamber used can be found in Figure 6-2 below:

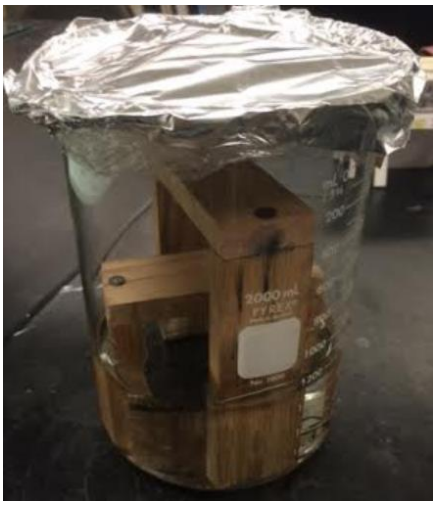

Figure 6-2. 100% relative humidity chamber.

Unlike the thermally aged samples, the samples subjected to the moisture degradation condition did not appear to have any visual changes.

6.2 Raw Data: Thermally Aged Specimens

Following the same procedure as the as-is samples, pressure versus displacement data was collected for each sample. During the test, samples failed either via delamination or brittle fracture; the latter was removed from the set analyzed. It is important to note that the as-is samples never failed via brittle fracture, further suggesting a change in material properties. Finally, visual inspection of the raw data suggests that the thermal aging

increased the stiffness of the material tremendously when compared to the as-is case. Critical heights are magnitudes of order smaller than as-is samples even though critical pressures are orders of magnitudes larger. Based on this, it is reasonable to hypothesize a significant increase in modulus. A summary of the collected data can be seen below in Table 6-1**.** The plots of the raw data can also be seen below in Figure 6-3.

Table 6-1. Summary of thermally aged testing data.

Sample	**Thickness (mm)**	**Critical Pressure (psi)**	**Critical Height (mm)**
13	0.270	48.7	0.052
14	0.220	44.9	0.050
15	0.376	87.9	0.023
16	0.370	49.8	0.010
17	0.340	63.5	0.031
18	0.329	62.4	0.027
19	0.334	64.8	0.040
20	0.360	82.7	0.028
21	0.322	68.0	0.017
22	0.372	80.7	0.015

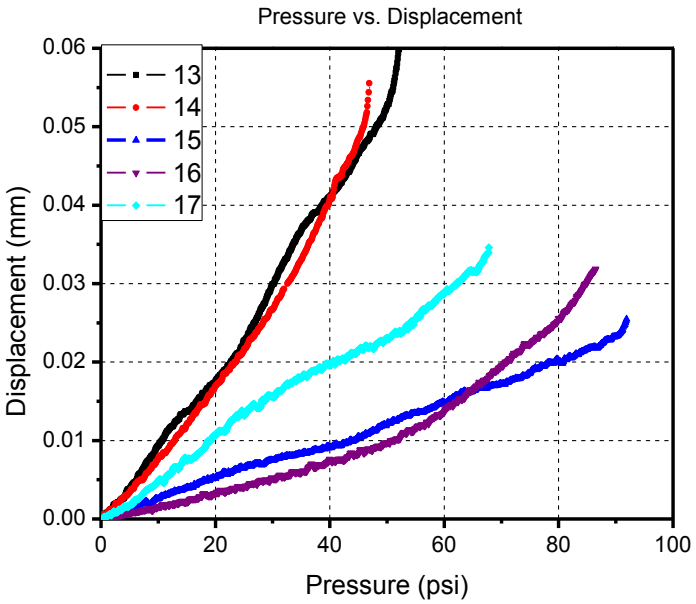

(a)

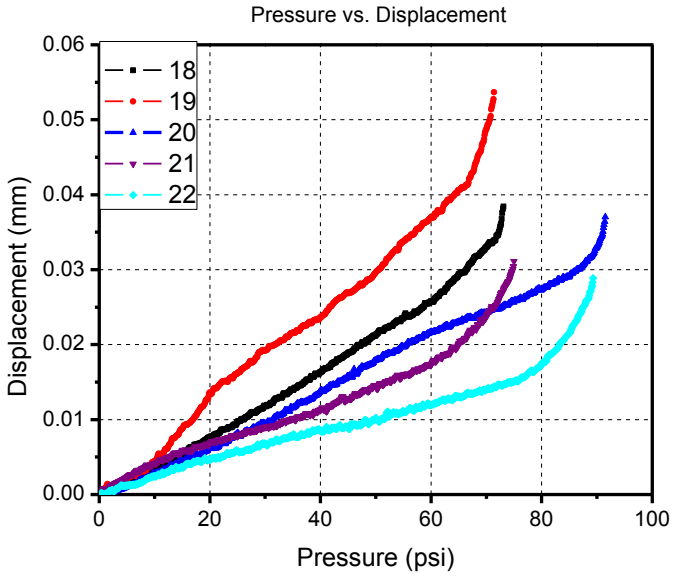

(b)

Figure 6-3. Raw data from thermally aged tests for samples (a) 13-17, and (b) 18-22.

6.3 Raw Data: Moisture Degraded Specimens

Following the same procedure used for the as-is and thermally aged samples, the moisture degraded samples were subjected to the advanced blister test. During the tests, all samples failed via delamination. Visual inspection of the data shows failure at a much smaller critical pressure and critical height, indicating the possibility of decreased adhesion strength. A summary of the data can be seen below in Table 6-2. Additionally, the plots of the raw data are found in Figure 6-4. .

Table 6-2. Summary of moisture degraded testing data.

Sample	Thickness (mm)	Critical Pressure (psi)	Critical Height (mm)
23	0.271	12.60	0.180
24	0.220	8.70	0.112
25	0.319	7.80	0.061
26	0.294	11.90	0.050
27	0.257	9.90	0.083
28	0.255	8.20	0.070

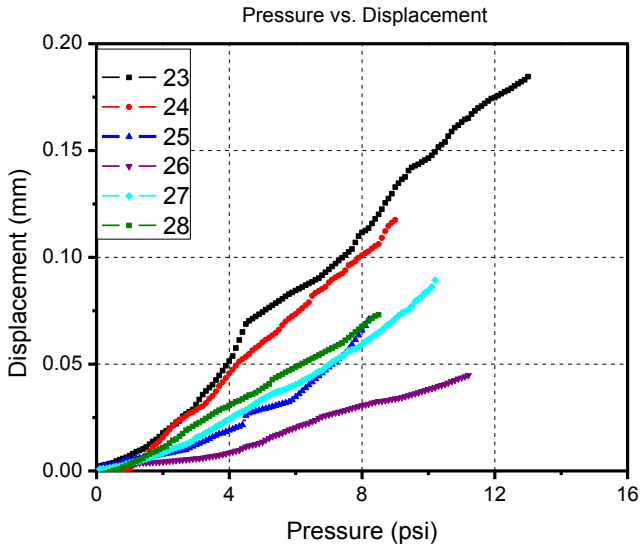

Figure 6-4. Raw data from moisture degraded tests.

6.4 Analysis of Data: Thermally Aged Specimens

The data obtained was analyzed via the method described in sections 5.2 and 5.3 to obtain the pseudo-modulus and energy release rate for each blister specimen. The results can be found below in Table 6-3**.**

Table 6-3. Thermally aged specimen results after analysis.

Sample	**Thickness (mm)**	**Critical Pressure (psi)**	**Critical Height (mm)**	**Calculated Pseudo-E (GPa)**	**Calculated G (J/m^2)**
13	0.270	48.7	0.052	28.5	26.68
14	0.220	44.9	0.050	58.0	40.52
15	0.376	87.9	0.023	49.7	19.55
16	0.370	49.8	0.010	67.8	11.52
17	0.340	63.5	0.031	32.2	18.60
18	0.329	62.4	0.027	39.8	20.01
19	0.334	64.8	0.040	27.2	45.77
20	0.360	82.7	0.028	38.3	20.72
21	0.322	68.0	0.017	73.8	23.15
22	0.372	80.7	0.015	67.2	18.47

Initial observation of the pseudo-modulus calculations suggest that while they are much larger than the as-is case, there is large scatter and instability with this material property after thermal aging. The calculated energy release rates appear to be within range of those of the as-is case.

6.5 Analysis of Data: Moisture Degraded Specimens

The data collected for the moisture degraded specimens was also analyzed via the method previously mentioned. The results are listed in

Table 6-4**.**

Table 6-4. Moisture degraded specimen results after analysis.

Sample	**Thickness (mm)**	**Critical Pressure (psi)**	**Critical Height (mm)**	**Calculated Pseudo-E (GPa)**	**Calculated G (J/m^2)**
23	0.271	12.60	0.180	2.00	26.44
24	0.220	8.70	0.112	4.20	12.82
25	0.319	7.80	0.061	2.30	8.47
26	0.294	11.90	0.050	5.50	10.61
27	0.257	9.90	0.083	4.10	12.82
28	0.255	8.20	0.070	4.60	8.57

A quick observation shows that the pseudo-modulus values appear to be within range of those from the as-is case whereas the energy release rate values seem to be significantly reduced.

6.6 Statistical Comparison Between As-is and Thermally Aged Samples

To quantify the differences or similarities between data sets, statistical analysis is used. The goal of this analysis is to determine whether or not the pseudo-modulus and energy release rates are statistically identical between the two groups of data. First, the average and standard deviation of the pseudo-modulus and energy release rate are calculated. These values are found below and compared with the as is case in Table 6-5**.**

Table 6-5. Comparison of results between as-is and thermally aged samples.

Parameter	**Mean**	**Standard Deviation**
Pseudo-Modulus (as-is)	3.58 GPa	1.12 GPa
Energy Release Rate (as-is)	34.15 J/m^2	4.96 J/m^2
Pseudo-Modulus (thermally loaded)	48.25 GPa	17.49 GPa

Energy Release Rate (thermally loaded)	24.50 J/m^2	10.07 J/m^2

The two null hypotheses become:

$$\mu_{E,as-is} = \mu_{E,aged} \tag{5.1}$$

$$\mu_{G,as-is} = \mu_{G,aged} \tag{5.2}$$

Analysis of this type is best adapted for ANOVA (analysis of variance) or Kruskal-Wallis tests. Both allow us to make a conclusion about whether the null hypotheses should be accepted or rejected. The underlying difference between the two tests, however, is the assumptions made about the distribution of the population from which experimental data is obtained. The ANOVA test assumes that the population follows a normal distribution whereas the Kruskal-Wallis test does not make an assumption. Despite this advantage, the Kruskal-Wallis test is considered to be less accurate than ANOVA since it relies on data ranking as a method of analysis. The distributions of the normalized data are analyzed using the Kolmogorov-Smirnov test for normality. The results from this test can be found below in Table 6-6**.**

Table 6-6 Results from test for normality

Parameter	**Normality Test p-value**
Pseudo-Modulus (as-is)	0.2061
Energy Release Rate (as-is)	0.9356
Pseudo-Modulus (thermally aged)	0.8214
Energy Release Rate (thermally aged)	0.2424

Using α=0.10, it can be concluded that all sets of data follow a normal distribution, making the one way ANOVA test most applicable for analysis between samples means. A summary of the p-values obtained from this analysis can be found below in Table 6-7**.**

Table 6-7. Summary of p-values for comparison of thermally aged sample set.

Parameter	One Way ANOVA Test p-value
Pseudo-Modulus	2.28e-8
Energy Release Rate	0.0636

Using α=0.10, it is evident that both the null hypotheses (equations 6-1 and 6-2) should be rejected. After thermal aging, the pseudo-modulus of F114 increased significantly whereas the energy release rate decreased significantly.

6.6 Statistical Comparison Between As-is and Moisture Degraded Samples

A procedure similar to section 6.5 is followed to compare the as-is and moisture degraded specimens. First, the mean and standard deviation values for the energy release rate and pseudo-modulus are calculated below in Table 6-8.

Table 6-8. Comparison between as-is and moisture degraded samples.

Parameter	Mean	Standard Deviation
Pseudo-Modulus (as-is)	3.58 GPa	1.12 GPa
Energy Release Rate (as-is)	34.15 J/m^2	4.96 J/m^2
Pseudo-Modulus (moisture degraded)	3.78 GPa	1.24 GPa
Energy Release Rate (moisture degraded)	13.29 J/m^2	6.14 J/m^2

Next, the distributions are checked for normality in Table 6-9 Results from test for normality below.

Table 6-9 Results from test for normality

Parameter	Normality Test p-value
Pseudo-Modulus (as-is)	0.2061
Energy Release Rate (as-is)	0.9356
Pseudo-Modulus (moisture degraded)	0.7339
Energy Release Rate (moisture degraded)	0.3314

Using α=0.10, we can assume normal behavior and the one way ANOVA test is used once again to test the following null hypotheses:

$$\mu_{E,as-is} = \mu_{E,moisture} \tag{5.3}$$

$$\mu_{G,as-is} = \mu_{G,moisture} \tag{5.4}$$

Finally, p-values are generated for each of the null hypotheses. These values are shown below in Table 6-10**.**

Table 6-10. Summary of p-values of moisture degraded sample set.

Parameter	One Way ANOVA Test p-value
Pseudo-Modulus	0.7456
Energy Release Rate	0.0014

Once again using α=0.10, it is evident that the pseudo-modulus values are not statistically different between the as-is and moisture degraded tests. The energy release rate, however, is statistically different. It can therefore be concluded that after exposure to moisture conditions, adhesion strength decreases but there is no influence on pseudo-modulus values.

6.7 Summary of Data

A graphical comparison of the calculated pseudo-modulus and energy release rate results for each test condition can be seen below in Figure 6-5 and Figure 6-6, respectively.

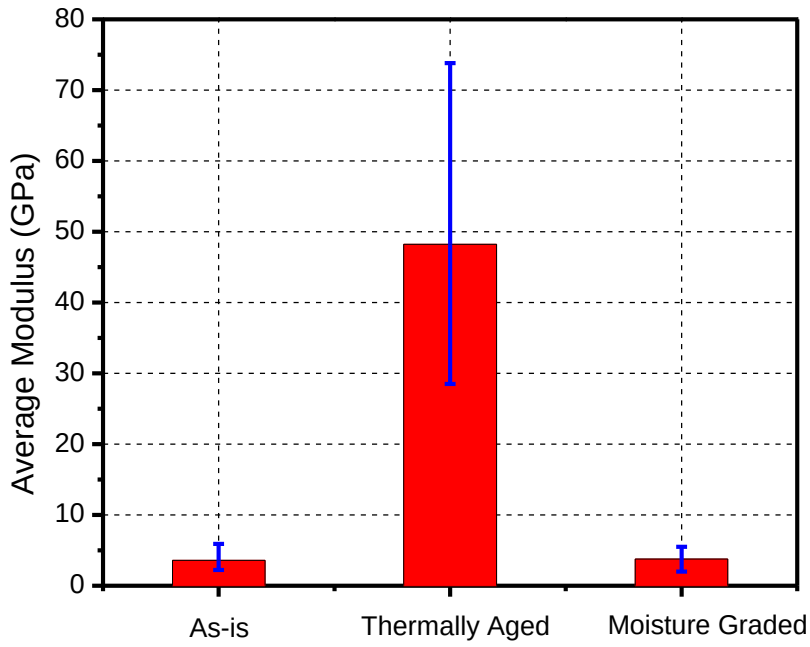

Figure 6-5. Average pseudo-modulus values and ranges for environmental conditions.

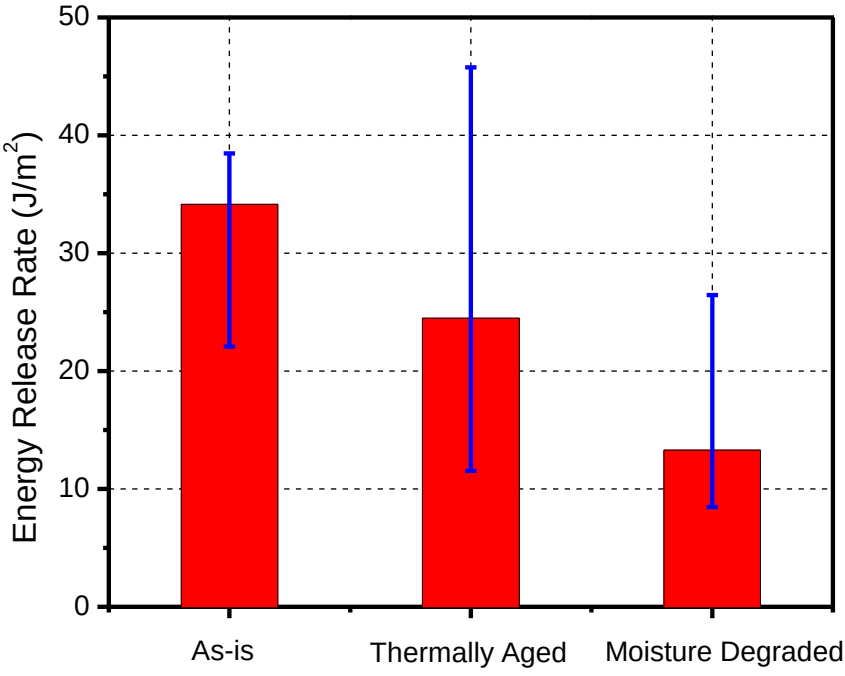

Figure 6-6. Average energy release rate values and ranges for environmental conditions.

CHAPTER 7: DISCUSSION

7.1 Instrument Resolution

After preloading the specimen to separate the predefined area, small plastic deformations are evident within the specimen. When the initial pressure load is stepped down to zero, random deflections are seen in the data. Data from six representative samples can be found below in Table 7-1**.**

Table 7-1. Deflection after initial loading of six samples.

Test	Specimen Thickness (mm)	Initial Displacement (mm)	Critical Height (mm)	Percentage of Critical Height
1	0.240	0.00258	0.143	1.8%
2	0.323	0.00311	0.104	3.0%
3	0.282	0.00660	0.162	3.9%
4	0.311	0.00381	0.119	3.2%
5	0.365	0.00693	0.098	7.1%
6	0.351	0.00341	0.107	3.2%

The manufacturer of the laser displacement sensor indicates that the instrument has a resolution of 0.00125 mm. Initially, it is clear that the initial displacements observed are larger than this resolution value suggesting that this displacement shouldn't be attributed to error from the instrument. To confirm the manufacturer's specification, the displacement was stepped from 0.5 mm to 0 mm repeatedly using an appropriately sized shim (see Figure 7-1). A maximum zero error of 0.001 mm was obtained after ten trials.

Figure 7-1. Verification of laser displacement sensor.

The manufacturer of the pressure regulator claims a resolution of 0.1 psi. An ANSYS model for each specimen is run to determine the displacement obtained should the pressure regulator provide a pressure of 0.1 psi instead of 0 psi. The calculated displacements were significantly less than the measured displacements for each case (see Table 7-2). Although small deformations can be confirmed, they are considered to be negligible and the analysis is run using the assumption of perfectly elastic material.

Table 7-2. Comparison of initial displacement to calculated values.

Test	Initial Displacement (mm)	ANSYS Calculated Displacement (mm)
1	0.00258	0.00175
2	0.00311	0.00059
3	0.00660	0.00122
4	0.00381	0.00077
5	0.00693	0.00048
6	0.00341	0.00047

7.2 Uncertainties in Thickness Measurements and Poisson's Ratio

Small errors in thickness measurements can have an impact on the accuracy of pseudo-modulus and energy release rate calculations. In the future, improvements in sample preparation to allow for a more perfect and uniform blister surface could reduce this potential error.

For all calculations, a Poisson's ratio of 0.4 is assumed for the F114 material. Inaccuracies in this assumption have a moderate impact on the calculated value for modulus. Despite this, the value calculated for energy release rate does not change with inaccurate Poisson's ratio values. Observing the analytical equations in chapter 2 for the bending and stretching cases, it can be seen that the pseudo-modulus and Poisson's ratio are coupled in such a way that inaccuracies in both of these values do not have an impact on the energy release rate. For both cases, there exists and infinite combination of the two properties that will produce identical results for energy release rate. Because of this, if the Poisson's ratio is assumed and fixed, the corresponding modulus (pseudo-modulus) value can be calculated and used for energy release rate calculations. Consistency for the mixed mode case is verified through FEM. The result of sample calculations showing the effect of Poisson's ratio on pseudo-modulus and energy release rate can be seen below in Table 7-3.

Table 7-3. Error in incorrect Poisson's ratio value.

Poisson's Ratio	**Pseudo-Modulus (GPa)**	**Percent Error**	**Energy Release Rate (J/m^2)**	**Percent Error**
0.20	84.4	12.6%	21.40	~0%
0.30	80.0	7.8%	21.40	~0%
0.35	77.2	4.4%	21.40	~0%
0.40	73.8	-	21.39	-
0.45	70.0	5.4%	21.38	~0%

CHAPTER 8: CONCLUSIONS

The advanced blister test with predefined area was proposed and implemented as a method to characterize adhesion strength between a polymer adhesive of unknown modulus and a rigid substrate. The predefined area allowed for a uniform and circular precrack area, yielding an axisymmetric circular plate with clamped edges configuration. In addition, the predefined area reduced the possibility of stress concentrations while loading, reducing the possibility of inaccurate results. With this configuration, the setup was accurately modeled using FEM software. Also, due to modifications in traditional blister sample preparation, the predefined area also had low adhesion allowing for low-pressure separation.

Due to the rate dependent nature of polymer materials, it was important to characterize the blister modulus in situ with the adhesion testing before calculating the energy release rate. Using a constant modulus could produce inaccurate results with varying blister thicknesses or configurations. Numerical modeling software allowed this task to be accomplished efficiently. After following the procedure, an average pseudo-modulus of 3.58 GPa and an average energy release rate of 34.15 J/m^2 were calculated for the as-is F114 samples.

In the experiments run, exposure to thermal aging and moisture caused a significant decrease in adhesion strength for the F114 and copper interface. Accelerating aging of the material above its glass transition temperature resulted in a sharp increase in the pseudo-modulus to an average of 48.25 GPa and decreased the overall adhesion strength to an

average of 24.50 J/m^2. Exposing the samples to 100% relative humidity had no effect on the pseudo-modulus but caused a drastic decrease in adhesion strength to an average of 13.29 J/m^2. Environmental aging, therefore, should be a primary concern when considering mechanical and adhesion properties of epoxy materials.

APPENDIX

Appendix A: Advanced blister test ANSYS model code:

```
! ********************model_2d ANSYS ********************
!  /input,'C:\ANSYS\Test Run Files\Blister\SBT_Setup',txt
! 2D Axisymetric Model
! This file has one film layer with a a bottom substrate
! Pressure loading is applied directly to the film layer.
! Setup model setus up all parameters except for the critical load and modulus
!*****************
! Properties that change
fini                                ! Start new session
/clear                              ! Clear out any saved parameters
h_film=0.351            ! mm
E_film=2500             !MPa
nu_film=0.4
!Delta_a_Step=0
version=1
!*****************
/filname,SBT_Model,db               ! Name the database
! Define Parameters (Units: N-mm-sec-K)
! Mesh Info
elm_thick=4
elm_size=0.1/4
ratio=5
tol=1e-6                                    ! Define a tolerance
h_sub=0.750
a_sub=2
a_PD=4.7625 !3/16"
Delta_a=elm_size*Delta_a_Step
a_radius=a_PD+Delta_a                       ! radius (a)
a_constraint=a_radius+1
length=a_constraint+1                       ! model_extent distance of substrate past a_radius
P_Max_psi=20  !0.001  ! psi
P_Max=P_Max_psi/146   !ramp*tspan               ! Maximum Pressure - in MPa
nstep=3 !20                                     ! Define number of steps to run
!  Geometry
x1=0
x2=a_sub
x3=a_radius
x4=a_constraint
x5=length
y1=0
y2=h_sub
y3=y2
```

```
y4=y3+h_film
z0=0
! ********************Preprocessing Section***************
/prep7
!  Create Element Types
et,1,183,,,1         ! PLANE183 is a 2d structural solid brick element (with axisymmetric
option)
! Define Material Properties
! 1: film, 2: Cover, 3: Si Substrate
mat_film=1
mat_sub=3
E_sub=110e3
nu_sub=0.3
ex,mat_film,E_film
nuxy,mat_film,nu_film
ex,mat_sub,E_sub
nuxy,mat_sub,nu_sub
!  Create Areas  (Use only half geometries due to symmetry)
k,13,x1,y3,z0
k,14,x1,y4,z0
k,21,x2,y1,z0
k,22,x2,y2,z0
k,23,x2,y3,z0
k,24,x2,y4,z0
k,31,x3,y1,z0
k,32,x3,y2,z0
k,34,x3,y4,z0
k,41,x4,y1,z0
k,42,x4,y2,z0
k,44,x4,y4,z0
k,51,x5,y1,z0
k,52,x5,y2,z0
k,54,x5,y4,z0
! Lines
a_elm=(x2-x1)/(elm_size*ratio)
b_elm=(x3-x2)/(elm_size*ratio)
c_elm=(x4-x3)/(elm_size*ratio)
d_elm=(x5-x4)/(elm_size*ratio)
e_elm=10
f_elm=h_film/elm_size
l,32,22,b_elm !1
l,31,21,b_elm !2
l,32,42,c_elm !3
l,31,41,c_elm !4
l,42,52,d_elm !5
l,41,51,d_elm !6
```

```
l,22,21,e_elm,5 !7
l,32,31,e_elm,5 !8
l,42,41,e_elm,5 !9
l,52,51,e_elm,5 !10
l,24,14,a_elm !11
l,23,13,a_elm !12
l,34,24,b_elm !13
l,32,23,b_elm !14
l,34,44,c_elm !15
l,44,54,d_elm !16
l,13,14,f_elm !17
l,23,24,f_elm !18
l,32,34,f_elm !19
l,42,44,f_elm !20
l,52,54,f_elm !21
!******************
! Areas
al,1,8,2,7  !1
al,3,9,4,8  !2
al,5,10,6,9 !3
al,11,18,12,17  !4
al,13,19,14,18   !5
al,15,20,3,19   !6
al,16,21,5,20   !7
asel,,loc,y,y1,y2
AATT,mat_sub,,1
asel,,loc,y,y2,y4
AATT,mat_film,,1
alls
! Meshing Section
alls
MSHKEY,1
MSHAPE,0,2D
amesh,all
alls
!*************************************************************
! Create Components
!**********
! Fix Y Displacement at Bottom of Substrate
nsel,r,loc,y,y1-tol,y1+tol
cm,nfix_y,node
! Fix X Displacement at Center of Model
nsel,,loc,x,x1-tol,x1+tol      ! Reselect indicated node locations with y=0 and that are at
bottom of substrate
```

```
cm,nfix_x,node                  ! CM used to define a component of the currently selected nodes, give it a name (nfix), which is comprised of a certain type of entity (node) where degree of freedom is fixed
! Fix X Displacement at Bottom Substrate behind Crack
nsel,,loc,x,x2-tol,x2+tol      ! Reselect indicated node locations with y=0 and that are at bottom of substrate
nsel,r,loc,y,y1-tol,y1+tol
cm,nfix_bot_x,node
! Component for Pressure at bottom of Film
nsel,,loc,y,y3-tol,y3+tol
nsel,r,loc,x,x1-tol,x3+tol
cm,P_area,node
! Component for Blister Height
nsel,,loc,y,y3-tol,y3+tol
nsel,r,loc,x,x1-tol,x1+tol
*get,nod_cent,node,,num,min
alls
*get,n_count,node,,count
!+++++++++++++++++++++++++++++++++++++++++++++++++++++++++++++++
alls
SAVE
```

Appendix B: Matlab Code for Modulus Solver

```
%% Set Optimization Parameters
% Searching for the Modulus in this Optimization Case
E_min = 2000; % MPa
E_max = 4000; %MPa
E_inc = 50; %MPa
converge = 0.0001; %Converge within 0.01% of R2 Value
Count_Max=round(E_max-E_min)/E_inc;
E_track=zeros(Count_Max,1);
w_err_track=zeros(Count_Max,1);
R2_track=zeros(Count_Max,1);
%% Experimental Data - Create Cubic Fit of Data
Exp_data = xlsread('ex_3b.csv');
P_exp = Exp_data(:,1);
w_exp = Exp_data(:,2);
[row,col] = size(w_exp);
w_avg=(1/row)*sum(w_exp);
%% Create baseline model and meshing
% Creates model that will be recalled in loop below
!"C:\Program Files\ANSYS Inc\v145\ANSYS\bin\winx64\ansys145.exe" -b -i
SBT_Setup.txt -o output.txt
```

```
%% Loop to Fit E_mod to experimental data
%Update Material Properties
% Takes P_max_psi as an input
P_max_psi = max(P_exp);
w_crit = max(w_exp);
   E_mod = E_min;  %MPa
for xx = 1:Count_Max


   % Create update file for ANSYS
   write_Mod = sprintf('E_mod = %d ', E_mod);
   write_P = sprintf('P_max_psi = %d ', P_max_psi);
   fileID=fopen('MatPropUpdate.txt','w');
   fprintf(fileID, 'RESUME,"SBT_Model",db,,0,1');
   fprintf(fileID, '\n');
   fprintf(fileID, write_Mod);
   fprintf(fileID, '\n');
   fprintf(fileID, write_P);
   fclose(fileID);
   % type MatPropUpdate.txt

   % Run Model with Updated Material Properties
   % Create output Pressure vs.  height file
   !"C:\Program Files\ANSYS Inc\v145\ANSYS\bin\winx64\ansys145.exe" -b -i
bt_test.txt -o output.txt

   A = xlsread('output_file.csv');
   P = A(:,1);
   w_num = A(:,2);
   [w_fit,gof] = fit(P,w_num,'poly3');

   w_err = 0;
   SS_reg = 0;
   SS_tot = 0;
   w_crit_ansys=w_fit(P_exp(row,1));
   for i = 1:row
      SS_reg = SS_reg + (w_exp(i,1)-w_fit(P_exp(i,1)))^2;
      SS_tot = SS_tot + (w_exp(i,1)-w_avg)^2;
      w_err = w_err + (w_fit(P_exp(i,1))-w_exp(i,1))/w_exp(i,1)*(w_crit/w_exp(i,1));
   end
      R2_value = 1 - SS_reg/SS_tot;

   %Record stats for run
   E_track(xx,1) = E_mod;
   w_err_track(xx,1) = w_err;
   R2_track(xx,1) = R2_value;
```

```
   if xx > 1
     conv_check = (R2_value - (R2_track(xx-1,1)));
     if conv_check < 0
        R2_value = R2_track(xx-1,1)
        E_mod = E_mod - E_inc;
        break
     end
   end

   E_mod = E_mod + E_inc;
end

plot(P_exp,w_exp,'.b')
hold on
plot(P_exp,w_fit(P_exp),'-r')

xlabel('Pressure (psi)');%  add axis labels and plot title
ylabel('Blister Height (mm)');
y_leg = legend('Experimental','Numerical Fit');

E_mod
```

Appendix C: Matlab Code for Energy Release Rate Solver

```
function G_actual = SBT_Evaluate_Fun(Sample_Number,h_film,E_film,P_Max_psi)
%% Solve Standard Blister Test ANSYS File and G
% SBT_Evaluate.m
%% Set case parameters for given experiment

% Sample_Number = 'test_3b';
% h_film = 0.323; % In mm
% E_film = 2850;  % In MPa
% P_Max_psi = 17.67; % In psi

nu_film = 0.4;
Delta_a_Max = 3;
a_PD = 4.7625;

%% Declare and Dimension Vectors
Vol = zeros(Delta_a_Max +1,1);
W=zeros(Delta_a_Max+1,1);
Delta_W=zeros(Delta_a_Max,1);
Delta_a=zeros(Delta_a_Max,1);
Delta_Vol = zeros(Delta_a_Max,1);
```

```
G=zeros(Delta_a_Max,1);

%% Setup and Solve ANSYS File
for aa = 0:Delta_a_Max
   % Create update file for ANSYS
   write_SNum = sprintf('Sample = "%s"', Sample_Number);
   write_Name = sprintf('Name = "%s_%d"', Sample_Number,aa);
   write_hF = sprintf('h_film = %d ', h_film);
   write_Ef = sprintf('E_film = %d ', E_film);
   write_nuf = sprintf('nu_film = %d ', nu_film);
   write_Da = sprintf('Delta_a_Step = %d ', aa);
   write_P = sprintf('P_Max_psi = %d ', P_Max_psi);
   write_aPD = sprintf('a_PD = %d ', a_PD);
   fileID=fopen('CaseUpdate.txt','w');
   %fprintf(fileID, 'RESUME,"SBT_Model",db,,0,1');
   %fprintf(fileID, '\n');
   fprintf(fileID, 'fini');
   fprintf(fileID, '\n');
   fprintf(fileID, '/clear');
   fprintf(fileID, '\n');
   fprintf(fileID, write_SNum);
   fprintf(fileID, '\n');
   fprintf(fileID, write_Name);
   fprintf(fileID, '\n');
   fprintf(fileID, write_hF);
   fprintf(fileID, '\n');
   fprintf(fileID, write_Ef);
   fprintf(fileID, '\n');
   fprintf(fileID, write_nuf);
   fprintf(fileID, '\n');
   fprintf(fileID, write_Da);
   fprintf(fileID, '\n');
   fprintf(fileID, write_P);
   fprintf(fileID, '\n');
   fprintf(fileID, write_aPD);
   fprintf(fileID, '\n');
   fclose(fileID);
   % type CaseUpdate.txt
   !"C:\Program Files\ANSYS Inc\v145\ANSYS\bin\winx64\ansys145.exe" -b -i
SBT_Solve.txt -o output.txt

   %% Find deflection profile for the film
   XvsUY_data = xlsread('XvsUY.csv');
   prof_F(:,1) = XvsUY_data(:,1);
   prof_F(:,2) = XvsUY_data(:,2);
```

```
    % Specify you conditions
    TF_F = all(prof_F(:,1:2)==0,2);
    % remove
    prof_F(TF_F,:) = [] ;
    % sort data
    prof_F = sortrows(prof_F,1);

    % Get Film Volume
    Vol(aa+1,1) = 2*pi*trapz(prof_F(:,1),prof_F(:,2));
    clear prof_F
end

%% Take output from ANSYS to Solve for G
% Must look from aa = 0 to Delta_a_Max
P_Max=P_Max_psi*0.00689475729;
output_file = sprintf('%s.csv',Sample_Number);
[R_data,R_header,all1]= xlsread(output_file);

W(:,1) = R_data(:,10);
Delta_a(:,1) = R_data(2:Delta_a_Max+1,6);
Delta_W(:,1) = W(2:Delta_a_Max+1,1)-W(1,1);
Delta_Vol(:,1) = Vol(2:Delta_a_Max+1,1)-Vol(1,1);

%compile output table for determining G
% G = -1000*(P_MPa*Delta_V-Delta_W_T)/(2*pi*Delta_a*a)
G(:,1) = -1000*(P_Max.*Delta_Vol(:,1)-Delta_W(:,1))./(2*pi*Delta_a(:,1).*a_PD);

%plot(Delta_a(:,1),G(:,1))

p = polyfit(Delta_a(:,1),G(:,1),1);
G_fit=p(1)*Delta_a(:,1)+p(2);
yresid=G(:,1)-G_fit(:,1);
SSresid = sum(yresid.^2);
SStotal = (length(G)-1) * var(G);
RSquared = 1 - SSresid/SStotal;
G_actual= p(2);


%% Create and Save Results Table
  Results_Tab = zeros(Delta_a_Max+1,16);
  Results_Tab(1:Delta_a_Max+1,1:10)= R_data(:,:);
  Results_Tab(1:Delta_a_Max+1,11)=Vol;
  Results_Tab(2:Delta_a_Max+1,12)=Delta_W;
  Results_Tab(2:Delta_a_Max+1,13)=Delta_Vol;
  Results_Tab(2:Delta_a_Max+1,14)=G;
  Results_Tab(Delta_a_Max+1,15)=G_actual;
```

```
   Results_Tab(Delta_a_Max+1,16)=RSquared;

   G_Header(1,1:10) = R_header(1,1:10);
   G_Header(1,11) =  cellstr('Vol');
   G_Header(1,12) =  cellstr('Delta_W');
   G_Header(1,13) =  cellstr('Delta_Vol');
   G_Header(1,14) =  cellstr('G_da');
   G_Header(1,15) =  cellstr('G');
   G_Header(1,16) =  cellstr('R^2 Value');


% Create Output File
save_file = sprintf('%s_G.xlsx', Sample_Number);
xlswrite(save_file,G_Header,1,'A1')
xlswrite(save_file,Results_Tab,1,'A2')
```

REFERENCES

1. Kendall, K., *Adhesion: Molecules and Mechanics.* Science, 1994. **263**(5154): p. 1720-1725.
2. Anderson, T.L., *Fracture mechanics : fundamentals and applications*. 1995, Boca Raton: CRC Press.
3. Vallin, O.J.K.L.U., *Adhesion quantification methods for wafer bonding.* MATERIALS SCIENCE AND ENGINEERING R REPORTS -LAUSANNE-, 2005. **50**(4-5): p. 109-165.
4. Chang, Y.-S.L.Y.-H.D.D., *The Constrained Blister - A Nearly Constant Strain Energy Release Rate Test for Adhesives.* The J. of Adhesion The Journal of Adhesion, 1989. **27**(4): p. 197-211.
5. Napolitano, M.J.C.A.M.A., *The Constrained Blister Test for the Energy of Interfacial Adhesion.* Journal of Adhesion Science and Technology Journal of Adhesion Science and Technology, 1988. **2**(1): p. 311-323.
6. Hartshorn, S.R., *Structural Adhesives : Chemistry and Technology*. 1986, New York: Plenum Press.
7. Mittal, K.L. *Adhesive Joints : Formation, Characteristics, and Testing*. 1984. New York: Plenum Press.
8. Charalambides, P.G.L.J.E.A.G.M.R.M., *A Test Specimen for Determining the Fracture Resistance of Bimaterial Interfaces.* J. Appl. Mech. Journal of Applied Mechanics, 1989. **56**(1): p. 77.
9. Timoshenko, S.W.-K.S., *Theory of Plates and Shells*. 1959, New York: McGraw-Hill.
10. Hinkley, J.A., *A Blister Test for Adhesion of Polymer Films to SiO2.* The Journal of Adhesion The Journal of Adhesion, 1983. **16**(2): p. 115-125.
11. Gent, A.N.L.L.H., *Blow-Off Pressures for Adhering Layers.* APP Journal of Applied Polymer Science, 1987. **33**(5): p. 1567-1577.
12. Williams, M.L., *The Stresses Around a Fault or Crack in Dissimilar Media.* SPIE milestone series., 1997. **138**: p. 145.
13. Hencky, H., *Zr. Math. PHys.* 1915. **63**: p. 311-317.